

Damping of the de Haas–van Alphen oscillations in the superconducting state of MgB₂

J. D. Fletcher and A. Carrington

H.H. Wills Physics Laboratory, University of Bristol, Tyndall Avenue, BS8 1TL, United Kingdom

S. M. Kazakov and J. Karpinski

Laboratorium für Festkörperphysik, ETH Zürich, CH-8093 Zürich, Switzerland

(Received 12 May 2004; published 6 October 2004)

The de Haas–van Alphen (dHvA) signal arising from orbits on the π Fermi surface sheet of the two-gap superconductor MgB₂ has been observed in the vortex state below H_{c2} . An extra attenuation of the dHvA signal, beyond those effects described in the conventional Lifshitz-Kosevich expression, is seen due to the opening of the superconducting gap. Our data show that the π band gap is still present up to H_{c2} . The data are compared to current theories of dHvA oscillations in the superconducting state which allow us to extract estimates for the evolution of the π band gap with magnetic field. Contrary to results for other materials, we find that the most recent theories dramatically underestimate the damping in MgB₂.

DOI: 10.1103/PhysRevB.70.144501

PACS number(s): 74.70.Ad, 74.25.Jb

I. INTRODUCTION

The existence of two distinct energy gaps in the superconducting state of MgB₂ has been demonstrated by a number of experiments, including: tunneling,¹ specific heat,^{2,3} magnetic penetration depth,⁴ and angle resolved photoemission spectroscopy.^{5,6} Although there have been indications of two, or multigap, effects in other materials,^{7,8} it is in MgB₂ where the behavior has been most thoroughly investigated. Band structure calculations⁹ have shown that the Fermi surface of MgB₂ consists of four sheets, mostly arising from the boron orbitals. Two quasi-two-dimensional sheets originate from the boron σ orbitals and two more isotropic honeycomb-shaped sheets from the boron π orbitals. Theoretical work^{10,11} has predicted that the superconducting energy gap is substantially larger on the σ sheets than on the π sheets (at zero field and temperature the two gaps have been measured to be $\Delta_\sigma \approx 78$ K and $\Delta_\pi \approx 29$ K).^{4,12}

Although there have been several studies which have accurately measured the temperature dependence of the two gaps,^{1,13,14} there has been much less work in establishing how they evolve with magnetic field. Theoretical work¹⁵ predicts that at high field, both gaps decrease toward zero at a common upper critical field (H_{c2}) value, although at lower field, Δ_π is depressed much more rapidly than Δ_σ , particularly for $H \parallel ab$.¹⁶ Experimentally, the only direct studies of this have been by point contact spectroscopy. It has been suggested¹⁷ that Δ_π goes to zero at ~ 1 T (for $H \parallel c$), which is much lower than H_{c2} , although others^{18,19} have concluded that Δ_π remains finite above 1 T but becomes increasingly difficult to resolve because of scattering. In this paper, we use de Haas–van Alphen (dHvA) measurements as a probe of the gap in high magnetic fields. Our data clearly show the presence of a gap on one π -band sheet right up to the “bulk” H_{c2} .

The existence of dHvA oscillations in the superconducting state has been the subject of study for a number of years, and has been observed in a number of different materials: NbSe₂ (Ref. 20), V₃Si (Ref. 21), Nb₃Sn (Ref. 22), κ -(ET)₂Cu(NCS)₂ (Ref. 23), YNi₂B₂C (Ref. 24), and several

heavy fermion compounds.^{25–29} The effect is usually thought to arise through the overlap of quasiparticle states outside the vortex core. The amplitude of the oscillations is governed by the magnitude of the field dependent superconducting energy gap. In theory, the effect can be used to resolve the gaps on different Fermi surface sheets and to probe the field dependence of these gaps. However, in the current study scattering restricts our study to only one Fermi surface sheet.

The amplitude of the dHvA oscillations is interpreted using the Lifshitz-Kosevich equation for the oscillatory torque Γ of a three-dimensional Fermi liquid. The amplitude of the first harmonic is given by^{30,31}

$$\Gamma_{\text{osc}} \propto \frac{B^{3/2}}{[\Lambda'']^{1/2}} \frac{dF}{d\theta} R_D R_T R_S R_{SC} \sin \left[\frac{2\pi F}{B} + \varphi \right]. \quad (1)$$

Here the dHvA frequency F is related to the extremal area (Λ) of the orbit in k -space by $F = (\hbar/2\pi e)\Lambda$, $\Lambda'' = \partial^2 \Lambda / \partial k^2$ is the curvature factor and φ is the phase. The factor $R_T = X/(\sinh X)$ where $X = (2\pi^2 k_B / \hbar e)(m^* T/B)$, accounts for the effects of thermal broadening of the Landau-levels. It is from this temperature dependent term that the quasi-particle effective mass m^* is determined. The Dingle factor accounts for the effect of impurities and is given by $R_D = \exp(-\pi/\omega_c \tau)$, where $\omega_c = eB/m_B$, m_B is the unenhanced band mass^{30,31} and τ is the scattering time. The spin splitting factor R_S accounts for the reduction of amplitude caused by beating between the spin-up and spin-down Fermi surfaces. It is given by $R_S = \cos[\pi n g m_B (1+S)/2m_e]$ where S is the orbitally averaged exchange-correlation (Stoner) enhancement factor, g is the electron g -factor, m_e is the free-electron mass, and n is an integer. The final factor R_{SC} parametrizes the effect of superconductivity on the dHvA amplitude. It is this factor which is the primary focus of the current work and will be described more fully below.

The calculated Fermi surface of MgB₂, with predicted^{32–34} dHvA orbits, is shown in Fig. 1. We denote the frequency of each orbit n at a general angle by F_n . Previous studies^{35,36} have succeeded in observing orbits 1 to 6, thus verifying the topology of the calculated Fermi surface. The

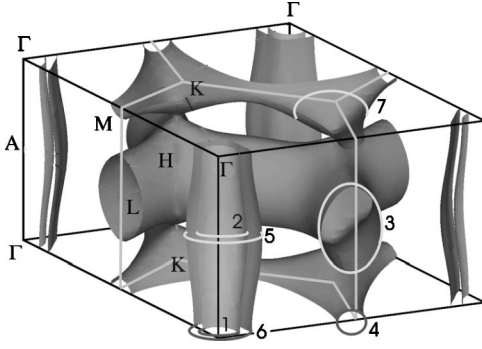


FIG. 1. Fermi surface of MgB₂ with predicted dHvA orbits (for frequencies less than 10 kT). In the present study, orbit 3 is the only one observable in the superconducting state. [Figure adapted from Kortus *et al.*⁹]

measured k -space areas of the orbits and the quasiparticle effective masses were found to be in good overall agreement with the calculations.^{32–34} Orbit 7 (Ref. 32) was not observed experimentally, perhaps because of a slight departure of Fermi surface topology from the calculations, or alternatively because of increased scattering on this orbit.

The relative amplitude of the various orbits is somewhat sample dependent. We have found that the mean-free-paths for different orbits does not change in a uniform way between samples.³⁶ Orbits 1–3 have by far the largest amplitude for fields below 20 T. The frequencies of these orbits all vary approximately like $1/\cos\theta$ (or $1/\sin\theta$), although for F_1 and F_2 there are some departures from this simple behavior due to the warping of the σ band sheet (see Ref. 35 for details). The amplitude of orbits 1–3 as a function of angle θ as the magnetic field is rotated from $B\parallel c(\theta=0)$ to $B\parallel a(\theta=90^\circ)$ is shown in Fig. 2. The strong angular dependence of H_{c2} , combined with the exponential attenuation of the signal by the Dingle factor, limits the range of angles where we are

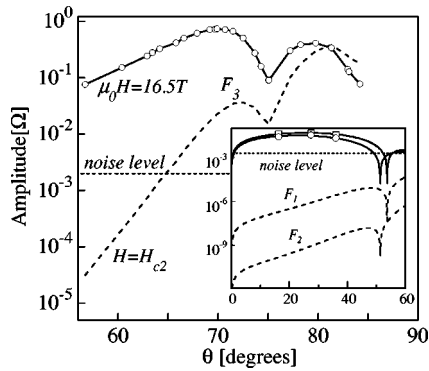


FIG. 2. The main figure shows the amplitude of the oscillations for orbit 3 at 16.5 T (symbols) as a function of angle (θ) (the solid line is a guide to the eye). The dashed line shows the extrapolated amplitude at $H=H_{c2}(\theta)$ using the measured Dingle factor R_D . The inset shows the corresponding angular dependence of the amplitude of orbits 1 and 2 at 16.5 T fitted according to Eq. (1) (solid lines), and the extrapolation to $H=H_{c2}(\theta)$ (dashed lines). The noise level of our measurement circuit is indicated on both parts of the figure. The mean-free-paths were measured to be 500, 610, and 840 Å for F_1 , F_2 , and F_3 , respectively.

able to observe oscillations below H_{c2} to $66^\circ \leq \theta \leq 81^\circ$ for the present crystals. The amplitude of the signal from orbits 1 and 2 at H_{c2} (Fig. 2 inset) is many orders of magnitude below our noise level, and so our study is limited to orbit 3 on the electron-like π sheet. We estimate that the mean-free-path ℓ would have to be approximately three times larger on orbit 1 for us to be able to see these oscillations at $\mu_0 H = 4$ T (for these crystals $\mu_0 H_{c2} \approx 4.3$ T at $\theta = 30^\circ$, although this does decrease with increasing ℓ [Ref. 36]).

II. EXPERIMENTAL DETAILS

Rather than measure the oscillations in the magnetic susceptibility, as in a conventional field modulated dHvA experiment, we have used miniature piezoresistive cantilevers³⁷ to measure the oscillations in the torque. We have found that this latter technique is significantly more sensitive than the former for the small size of the available high quality crystals of MgB₂.

The MgB₂ crystals were fixed with epoxy to the end of a boron-doped silicon cantilever about 150 μm long. Deflections in the cantilever were measured through the strain-induced changes in its electrical resistance, using an ac bridge technique. The torque values are reported here in units of bridge resistance R , i.e. the off-balance voltage divided by the excitation current (the change in cantilever resistance is $4R$). We estimate, using the weight of the sample, that $\Gamma \approx 10^{-10}R$ (Γ in Nm and R in Ω). The noise limit is around 2 m Ω or $\sim 10^{-13}$ Nm. In addition to the changes in resistance caused by the torque there is a small monotonic magnetoresistance of the sensor which we have not attempted to correct for.

The cantilever is mounted on a single axis rotation stage in a ³He cryostat inside the bore of a 19 T superconducting magnet (20.5 T at $T=2.2$ K). Unless otherwise stated, all measurements in this paper were performed in liquid ³He at 320 ± 20 mK. The orientation of the cantilever mount is detected using a pickup coil and a small modulated field collinear with the dc field. The small offset between the crystal plane and the cantilever mount was corrected using the symmetry of the dHvA frequencies around the $\theta=0^\circ$ and 90° points giving an uncertainty in the out of plane angle of $\pm 0.2^\circ$ (at $\theta \approx 90^\circ$). The in-plane orientation of the crystal ϕ (measured from the a -axis) is fixed for each run and measured by optical photographs and Laue x-ray diffraction (to $\pm 5^\circ$). A more precise determination of ϕ was made by comparing the minimum in the frequency of orbit 3 as a function of θ to the known frequency for this orbit at $\theta = \phi = 0^\circ$, as measured on a large number of other crystals³⁸ (the minimum frequency varies approximately as $1/\cos\phi$).

The torque, both due to the oscillations and the background magnetism, causes a deflection of the lever, and so θ is not quite constant during the field sweep. Using the strong angular dependence of the dHvA frequencies, we are able to measure the correspondence between the measured torque signal and the angular deflection of the cantilever. We find that the deflection is given by $\Delta\theta = (0.05 \pm 0.01)^\circ / \Omega$, which is approximately four times smaller than the value estimated from the manufacturer's data sheet.³⁷ This "torque interac-

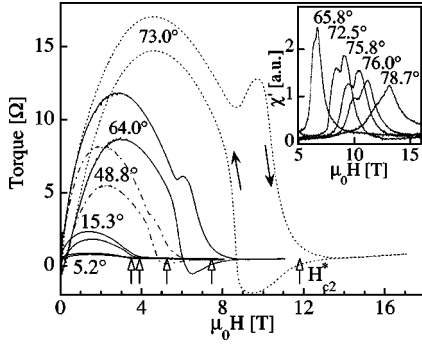


FIG. 3. Torque versus field at several values of θ at $T = 320$ mK. Both up and down field sweeps are shown. Inset: AC susceptibility (real part) versus field for different crystals from the same batch (at $T = 1.2$ K). The excitation field was 38 Oe at a frequency of 72 Hz.

tion" effect gives rise to spurious harmonics and mixing of the main frequencies. As the amplitude of the signal is also angle dependent (see Fig. 2) the field dependence of the signal will not exactly follow Eq. (1). Fortunately, this effect is small enough to be neglected for the purposes of the current work. This was verified by measuring samples with different masses and comparing up and down field sweeps (see later).

The samples used in this work were grown by a high pressure synthesis route as described in Ref. 39. Most of the work reported here was conducted on a crystal measuring $300 \times 160 \times 30 \mu\text{m}^3$ (mass = $3.9 \mu\text{g}$). The T_c of samples from this batch (AN77) was measured to be 38.5 K.

III. RESULTS

In Fig. 3 we show the measured torque versus field over a large range of field for a small sample from the same batch as our main crystal (mass = $0.4 \mu\text{g}$). This small sample was selected for this part of the study to avoid overstressing the cantilever. The general shape of the curve, a bell-shaped bump with a peak at around $H_{c2}/2$, has been explained theoretically in Ref. 40. Near H_{c2} there is evidently a pronounced peak effect which grows in size as the angle is increased. In addition, there is a significant region above the peak effect region where the torque is sizeable and remains hysteretic. Similar features have been reported previously by Angst *et al.*^{41,42} in their torque study of MgB_2 single crystals. Their study was conducted at higher temperature and lower field than the current work, and the peak effect they observed was less marked. In the inset to Fig. 3 we show data for the ac susceptibility of another crystal from the same batch (mass = $17 \mu\text{g}$). Many of the same features evident in the torque data are also visible here, namely, the broad superconducting transition and the pronounced peak effect.

The existence of a pronounced curvature in the region of the normal/superconducting transition along with the peak effect feature means that there is no unambiguous way of extracting H_{c2} from the measured torque curves. The rounding of the transition is common in high T_c materials where it is usually attributed to the presence of thermal or quantum fluctuations, which are enhanced relative to conventional low

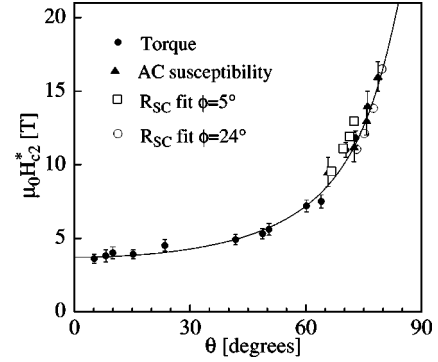


FIG. 4. H_{c2}^* as determined by torque measurements and ac susceptibility measured at 320 mK (solid symbols), along with a fit to Eq. (2). The open symbols show the values of $H_{c2}^*(\theta)$ extracted from the fits of R_{SC} using Eq. (3) for two different values of ϕ and are discussed later.

T_c materials due to the low dimensionality and high T_c of the former. MgB_2 is not strongly anisotropic, but has a relatively high H_{c2} (for H parallel to the basal plane) and hence small coherence lengths. The existence of hysteresis in this rounding region however, points to an explanation either in terms of surface superconductivity⁴³ or an as yet unexplained two gap effect, rather than fluctuations. It may also be possible that it could result from crystal inhomogeneity, although this is unlikely as reproducible behavior is found in crystals from the same batch.

We find that the angular dependence of H_{c2} derived by various extrapolation schemes (e.g., position of peak effect maximum or a linear extrapolation from low field) gives different absolute values, but essentially the same form for $H_{c2}(\theta)/H_{c2}(\theta=0)$ (the same conclusion was found by Angst *et al.*⁴²). As we shall see later, the onset of damping of the dHvA oscillations essentially coincides with a critical field H_{c2}^* derived by extrapolating the low field behavior, and so it seems likely that this represents the bulk upper critical field, at least for the π band.

In Fig. 4 we show values of H_{c2}^* extracted from the torque data in Fig. 3. These values are in good agreement with those extrapolated from higher temperature studies.⁴¹ In this figure we also show H_{c2}^* extracted from ac susceptibility data (inset to Fig. 3) in a similar way.

In an anisotropic superconductor the angular dependence of H_{c2} is usually described by

$$H_{c2}(\theta) = \frac{\gamma_H^2 H_{c2}^{||c}}{(\gamma_H^2 \cos^2 \theta + \sin^2 \theta)^{1/2}}, \quad (2)$$

where γ_H is the anisotropy of H_{c2} . In MgB_2 , the contribution of multiple Fermi surface sheets with different superconducting gaps is known to cause γ_H to increase with decreasing temperature and to cause deviations from the angular dependence predicted Eq. (2).⁴² However, these are small on the scale of Fig. 4, and are most pronounced near $\theta = 90^\circ$. A fit of Eq. (2) to the data is shown as a solid line in Fig. 4 ($\gamma_H = 7 \pm 0.5$ and $\mu_0 H_{c2}^{||c} = 3.7 \pm 0.3$ T).

Torque versus field for our main crystal is shown in Fig. 5 for three angles ($\theta = 63.8^\circ, 69.7^\circ, \text{ and } 72.5^\circ$). At these angles

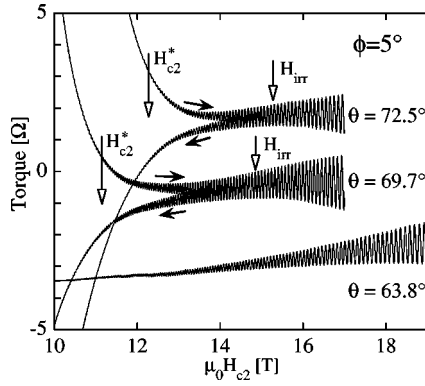


FIG. 5. Raw torque versus field close to H_{c2} for several angles θ .

only one dHvA frequency (F_3) is visible in our field range. For $\theta=69.7^\circ$ pronounced hysteresis is observable which disappears at an irreversibility field $\mu_0 H_{\text{irr}} \approx 15.5$ T. There is a small residual field dependence in the background torque which extends to ~ 16 T. We note that both these fields are far in excess of our estimate of H_{c2} obtained from the raw torque ($\mu_0 H_{c2}^* \approx 11$ T). Similar behavior can be seen for $\theta = 72.5^\circ$.

The field dependent amplitude A of the dHvA oscillations was extracted by fitting $A \sin(2\pi F_3/B + \varphi) + aB + b$ (the linear term accounts for the background torque) to different sections of data comprising of $1\frac{1}{2}$ oscillations. The data were then divided by the weakly field dependent term $B^{3/2}R_T$ to give $\tilde{A} \propto R_D R_{\text{SC}}$ [see Eq. (1)]. The quasiparticle effective mass m^* in the expression for R_T was determined by measuring the temperature dependence of the dHvA amplitude [for F_3 , $m^* = (0.456 \pm 0.005)m_e$ at $\theta = 70.8^\circ$].

In Fig. 6 we show \tilde{A} versus inverse field on semi-log axes (“Dingle plot”) for several angles. For $\theta=63.8^\circ$, \tilde{A} varies strictly exponentially with inverse field, $\tilde{A} \propto \exp(-74/B)$ from which we estimate that the quasiparticle mean free path on this orbit is 840 ± 20 Å. For this angle there is no evidence of superconductivity in either the background or oscillatory torque (see Fig. 5). As θ is increased H_{c2} increases sharply

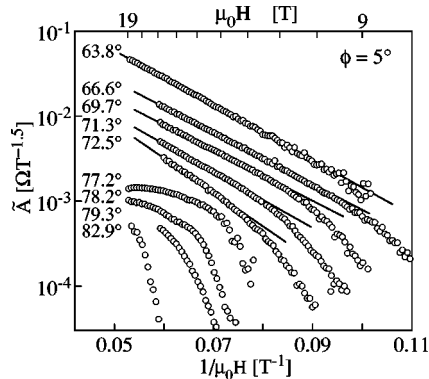


FIG. 6. Amplitude of dHvA oscillations divided by $B^{3/2}R_T$ versus inverse field, at several different values of θ [$\phi = 5^\circ$]. The data have been offset for clarity. The actual variation of amplitude with angle is shown in Fig. 2.

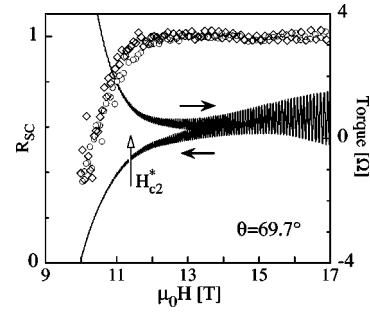


FIG. 7. Raw torque and superconducting damping, R_{SC} at $\theta = 69.7^\circ$, for both up and down field sweep directions (indicated by arrows).

and the Dingle plots have marked downturns below some critical field. We attribute this to the opening of the gap as the sample enters the superconducting state. To extract R_{SC} we fit $\tilde{A}(1/B)$ in the normal state to the exponential expression for R_D and extrapolate this dependence into the superconducting state (solid line in Fig. 6). Dividing \tilde{A} by R_D thus yields R_{SC} . An example of this is shown in Fig. 7 in which we also show the raw hysteretic torque. From this figure it can be seen that the onset of attenuation of the dHvA signal from R_{SC} does not occur until the field is below H_{irr} , and closely corresponds to the H_{c2}^* value (indicated by an arrow on Fig. 7) deduced by extrapolating the lower field data.

Most previous studies of the dHvA effect in the superconducting state have been conducted by the field modulation technique. In studies where this technique has been used the strong flux pinning close to H_{c2} (peak effect) has prevented data collection in this region. This did not present a serious problem as the oscillations could be observed far below H_{c2} [e.g., down to $H_{c2}/5$ in $\text{YNi}_2\text{B}_2\text{C}$ (Ref. 44) or $H_{c2}/2$ in V_3Si (Ref. 45)]. Studies of $\text{YNi}_2\text{B}_2\text{C}$ have shown that, in contrast to field modulation measurements, torque measurements⁴⁶ are not affected by this increased pinning. In MgB_2 , oscillations are only observable very close to H_{c2} and so all our measurements are essentially carried out in the peak effect region.

For ϕ near to 0° there is a pronounced dip found in the amplitude of the dHvA signal at $\theta \approx 75^\circ$ (see Fig. 8). This feature has been present in every crystal we have measured to date and always occurs when θ and ϕ are adjusted so that $F_3 \approx 2800$ T. Previously^{35,36} this feature has been attributed to a “spin-zero,” i.e., an angle where the angle dependent band mass multiplied by the Stoner factor exactly equals $m_e/2$, so that $R_S = 0$. However, a detailed analysis of the field dependence of the dHvA amplitude for angles above $\theta \approx 70^\circ$ reveals that in fact this dip is produced by a beat between two dHvA orbits with very similar frequencies. The inset to Fig. 8 shows Dingle plots close to $\theta \approx 75^\circ$. The data clearly show oscillatory beating damped by the Dingle factor (also visible in Fig. 6). A fit that takes account of this effect is shown for $\theta = 75.1^\circ$ in Fig. 8. The frequency difference is ~ 27 T at $\theta = 90^\circ$ and extrapolates to zero at $\theta = 70^\circ$ (for $\phi \sim 0^\circ$). The relative amplitudes of the two frequencies are almost equal over the whole angular range. The characteristics of this orbit are very similar to an additional orbit pre-

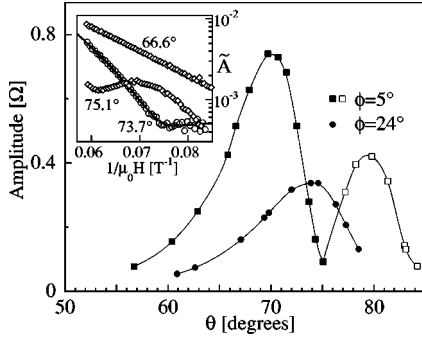


FIG. 8. Amplitude versus θ at $\mu_0 H = 16.5$ T, for two different in-plane rotation angles $\phi = 5^\circ$ and 24° the solid lines are guides to the eye. Open symbols are the amplitude at 18.5 T scaled by the appropriate Dingle factor. Inset: Dingle plots for θ near the minimum in amplitude at 75° (Data have been offset for clarity). The solid line on top of the data for 73.7° is a theoretical fit (see text).

dicted by Harima.³² A full account of this result will be given elsewhere.⁴⁷

A consequence of the above dip feature is that at angles close to or beyond $\theta \approx 75^\circ$ it is difficult to extract R_{SC} as the functional form of $\tilde{A}(1/B)$ is more complicated. For this reason we performed a second set of sweeps at a different in-plane angle ϕ . With $\phi = 24^\circ$, $F_3(\theta=0)$ is increased to 2930 T and thus the dip does not occur for any value of θ (see Fig. 8). In Fig. 9 we show the $\tilde{A}(1/B)$ curves for this in-plane angle.

As mentioned earlier, the deflection of the cantilever, either by the background or oscillatory torque, means that the fields sweeps are not done at strictly constant angle. As the dHvA amplitude is angle dependent this may cause some additional field dependence to \tilde{A} , which becomes large as the sample enters the superconducting state, and might cause error in our determination of R_{SC} . The insensitivity of our results for R_{SC} to this deflection is perhaps best demonstrated by comparing $\tilde{A}(1/B)$ curves for up and down field sweeps. In Fig. 10 we show both the raw torque signal and $\tilde{A}(1/B)$ for $\theta = 71.7^\circ$. There is a large difference in the background torque below H_{irr} in the two cases, which means that the sample is deflected in opposite directions (maximum deflection $\sim 0.7^\circ$), however it can be seen that the drop in $\tilde{A}(1/B)$

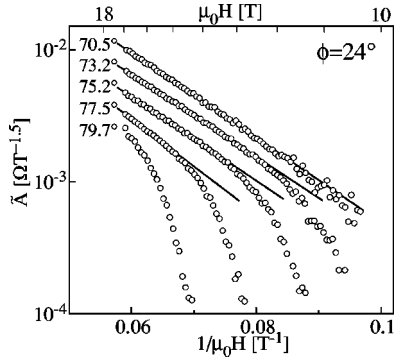


FIG. 9. Dingle plots for in-plane rotation $\phi = 24^\circ$. The solid lines are fits to the Dingle factor R_D [Eq. (1)] for the data above H_{c2} .

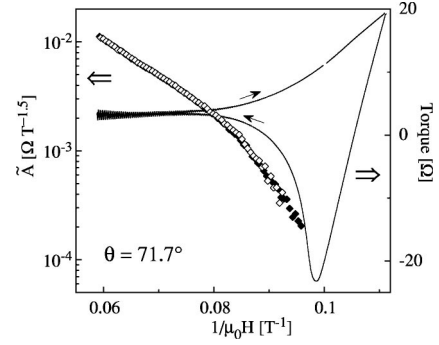


FIG. 10. Raw torque and \tilde{A} versus inverse field at $\theta = 71.7^\circ$ for both up and down field sweeps. The direction of the field sweep is indicated with the arrows.

below H_{c2} is virtually identical (see also Fig. 7). As a further check we have repeated some of our measurements on a fragment of crystal cut from our main sample which had mass of only $1.3 \mu\text{g}$ ($\approx 0.3 \times$ mass of main sample). We found identical behavior, showing again that the lever deflection does not affect our results. The close correspondence of the results for R_{SC} for up and down sweeps is also a strong indication that our data is not strongly affected by pinning in the peak effect region.

IV. EXTRACTING THE GAP FROM THE SUPERCONDUCTING STATE DAMPING FACTOR

dHvA oscillations in the superconducting state have been observed in many different materials, and in all cases the oscillations persist into the superconducting state with the same frequency as in the normal state but with reduced amplitude. As the dHvA amplitude depends exponentially on field, all the materials investigated to date are those with high H_{c2} values, and are not necessarily conventional. For example, NbSe_2 and Nb_3Sn , have recently been suspected of having an exotic gap structure.^{48,49} In some ways, MgB_2 is the best understood of all the materials where this phenomena has been observed to date, although its multiple energy gap structure may complicate the analysis.

Several theoretical models have been proposed to describe the effect (see Ref. 50 and references therein). Two theories have proved most successful in describing the data to date. Maki⁵¹ used a semiclassical approach following that of Brandt *et al.*,⁵² in which the gap is approximated by the spatially averaged value of Δ^2 and the magnetic field is considered to be uniform. For quasiparticles moving perpendicular to the magnetic field this model predicts that the excitation spectrum is gapless. It is this gaplessness which is the physical origin of the quantum oscillations. The extra damping in the superconducting state is given by

$$R_{SC} = \exp \left[-\pi^{3/2} \left(\frac{\Delta_E(B)}{\hbar \omega_c} \right)^2 \left(\frac{B}{F} \right)^{1/2} \right]. \quad (3)$$

In this expression, the *effective* field dependent energy gap $\Delta_E(B)$ is resolved to that on a particular quasiparticle orbit. An equivalent expression was also derived by different au-

thors starting from alternative physical pictures.^{31,53}

An alternative expression was derived by Miyake,⁵⁴ who considered the effect of incorporating the zero field BCS quasiparticle energy and occupation numbers into the usual Lifshitz-Kosevich theory. In the superconducting state the sharp step in the Fermi function is replaced with the BCS quasiparticle occupation function ($|u_k|^2$) whose width is set by the superconducting energy gap. This gives a more gradual emptying of Landau levels than in the normal state, and hence a reduced dHvA amplitude. The size of the damping factor in this model is given by

$$R_{SC} = xK_1(x), \quad x = 2\pi \frac{\Delta_E(B)}{\hbar\omega_c}, \quad (4)$$

where $K_1(x)$ is the Bessel function of the second kind. Miller and Gyorffy⁵⁵ have derived the same result starting from the Bogoliubov-de Gennes equations.

Studies in other materials have shown that $\Delta_E(B=0)$ extracted by fitting data to these expressions⁴⁵ does not always coincide with the known energy gap (Δ) measured by more conventional means (for example tunneling). The correspondence between Δ_E and the superconducting gap is different in each theory, and this may also be different for different materials. For example, Janssen *et al.*⁴⁵ found that for NbSe₂ the Maki model gave $\Delta_E/\Delta=0.63$ whereas the Miyake model gave $\Delta_E/\Delta=0.11$. For V₃Si, Δ_E/Δ was found to be 2.6 and 0.61 for the two models, respectively. It is generally found that the Maki model gives values for Δ_E which are much larger than the Miyake model.

To compare these theories with experiment we can take two approaches. The first is to assume a form for the field dependence of the effective gap and then fit Eq. (3) or Eq. (4) to $R_{SC}(B)$ directly. The second is to solve Eq. (3) or Eq. (4) for $\Delta_E(B)$ at each field point and then compare $\Delta_E(B)$ to the expected behavior. We shall show both methods below.

In the usual mean-field BCS theory we expect

$$\frac{\Delta_E^2(B)}{\Delta_E^2(0)} = 1 - \frac{B}{B_{c2}}. \quad (5)$$

However, the observed rounding of the superconducting transition means that $d\Delta/dH$ does not change discontinuously at H_{c2} and so a more appropriate expression is

$$\frac{\Delta_E^2(B)}{\Delta_E^2(0)} = \frac{1}{2} \left[\left(1 - \frac{B}{B_{c2}} \right)^2 + \alpha^2 \right]^{1/2} + \frac{1}{2} \left(1 - \frac{B}{B_{c2}} \right). \quad (6)$$

This form of $\Delta(B)$ was used by Clayton *et al.*²³ to account for the effect of superconducting fluctuations, as it interpolates the mean field result at low field to the form expected for a strongly fluctuating system near H_{c2} . The phenomenological parameter α sets the strength of the fluctuations. As it is not clear where the rounding of the superconducting transition in MgB₂ is caused by fluctuations, we will regard α as a phenomenological parameter which describes the rounding, rather than attributing to it for now any particular physical significance. In any case, the values of $\Delta_E(B=0)$ are mostly determined by the portion of the R_{SC} curve well below H_{c2} (i.e., the data for the higher values of θ).

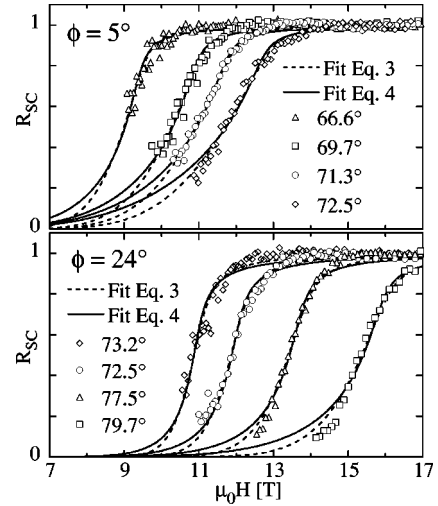


FIG. 11. R_{SC} for $\phi=5^\circ$ (top panel) and $\phi=24^\circ$ (bottom panel). The solid and dashed lines are fits to the Maki [Eq. (3)] and Miyake [Eq. (4)] theories for the superconducting state damping.

Combining Eq. (6) with either Eq. (3) or Eq. (4) results in three fitting parameters per curve [$\Delta_E(0)$, H_{c2} , and α]. We found that in general there was too much covariance between the parameters to arrive at accurate values for $\Delta_E(0)$ if we allowed all three to vary between the fits at each angle. As we do not expect either $\Delta_E(0)$ or α to vary strongly with θ we found that more consistent results were obtained by fitting to the data for $R_{SC}(B)$ at all angles simultaneously, only allowing H_{c2} to vary as a function of angle.

The fits obtained for both $\phi=5^\circ$ and $\phi=24^\circ$ are shown in Fig. 11. In these fits we have taken $m_B(\theta)=0.315m_eF_3/F_3^0$, i.e., assuming the band mass scales like the dHvA frequency.^{34,56} The values of $\Delta_E(B=0)$ and α are shown in Table I. It can be seen that both theories provide an adequate fit to the experimental data. The main difference is in the size of the extracted superconducting gap. As orbit 3 is on the electron like π sheet of Fermi surface we should compare these values with the zero field value for the smaller MgB₂ gap ($\Delta^s \approx 29$ K).⁴ The Miyake fit gives values comparable to this whereas the Maki fit gives values up to ten times larger. The trend is similar to that found for NbSe₂. The values of α are also somewhat larger in the Maki fits to those in the Miyake fits. The values of H_{c2} extracted from our fits are shown in Fig. 4. The values are very similar to those extracted from the background torque, consistent with our interpretation of our extrapolated H_{c2}^* as the bulk critical field for the π band. There is a consistent difference in $H_{c2}(\theta)$ values for the two values of ϕ , with the values for $\phi=5^\circ$

TABLE I. Parameters extracted from the fits to R_{SC} .

Theory	ϕ	$\Delta_E(B=0)$	$10^3 \times \alpha$
Maki	5°	200 ± 40 K	55 ± 10
Maki	24°	320 ± 40 K	34 ± 10
Miyake	5°	32 ± 10 K	27 ± 5
Miyake	24°	60 ± 10 K	22 ± 5

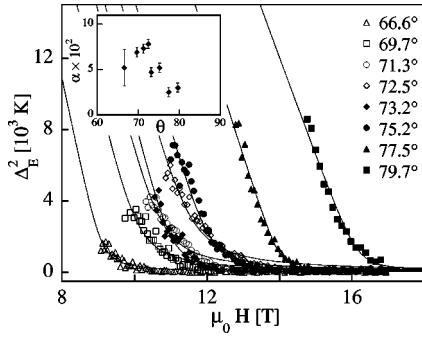


FIG. 12. Calculation of the field dependence of the superconducting gap, by inverting the R_{SC} curves in Fig. 11 using the Maki [Eq. (3)] model. The solid lines are fits to the field dependent gap [Eq. (6)] (see text). The inset shows the variation of the fit parameter α with θ .

being $\sim 10\%$ higher than those for $\phi=24^\circ$. This implies a slight in-plane anisotropy of H_{c2} .

Although there is some ambiguity between the theories as to the magnitude of the gap, it is clear that a sizeable gap does exist on this sheet of Fermi surface right up to H_{c2} . There is some difference between the gap values derived from the data at the two in-plane rotation angles. We note that although there is a large difference between the gaps on the σ and π Fermi surface sheets, the difference within a sheet (or indeed pair of sheets) is expected to be small.⁵⁷ One reason for this orientation dependence is that the data for $\phi=24^\circ$ cover a wider range of H/H_{c2} and hence, the extrapolated gap value is more accurate. For the runs with different ϕ where the H_{c2} values are close, the R_{SC} curves are very similar, and any difference results from the field range of the fit. Next, we show in Fig. 12 the field dependent effective gap calculated by inverting Eq. (3), along with fits to the field dependent gap given by Eq. (6). The main difference between using Eq. (4) rather than Eq. (3) is just in the magnitude of the extracted Δ_E rather than its field dependence. In the fits we have fixed $\Delta_E(B=0)$ to 300 K for all values of θ and ϕ and allowed α to vary. The curvature near H_{c2} and the approximately linear behavior of $\Delta_E^2(B)$ at lower field are evident. The covariance between the gap and H_{c2} mentioned above arises from the rounding at the transition and the small field range available at some angles. There is however a discernible progressive change in shape of the $\Delta_E(B)$ curves as θ and ϕ are varied. This is reflected in the angular dependence of α in the inset to the figure. This may be an artifact of the data analysis but could also result from a two gap effect.

It is clear that the extrapolation to the zero field gap is not a trivial one as our data does not extend below $0.85H_{c2}$. This is particularly significant in a material like MgB_2 , where nonmean-field gap behavior is expected. Numerical calculations^{15,16} of the field dependence of the energy gaps in MgB_2 show that they differ considerably from the mean field behavior given by Eq. (5). Close to H_{c2} , for $H\parallel ab$, we find that the numerical data can be approximated by $\Delta_\pi^2(B) = 0.24\Delta_\pi^2(0)(1-H/H_{c2})^{1.4}$. This accounts naturally for some (but not all) of the rounding in our R_{SC} plots. The steep drop

of Δ_π^2 at low field found in the calculations means that a linear extrapolation from high field underestimates the true zero field gap by approximately 50%, and the quantitative disagreement with the theory is even larger. There is also the possibility that the strong field dependence of the gap shown in Fig. 12 does not continue to low field but rather saturates rapidly below $H/H_{c2} \sim 0.85$. Given the above-mentioned theoretical work and the low field point contact spectroscopy results this would seem to be unlikely but cannot presently be discounted.

Recently, there has been further theoretical work on the dHvA effect in superconductors. Duncan and Gyorffy⁵⁸ have extended the work in Ref. 55 and given a new formula for R_{SC} . We have fitted our data to this formula and find fits that are comparable in quality to those in Fig. 11, with $\Delta_E(B=0) = 200 \pm 20$ K, for $\phi=5^\circ$. This is very close to the values calculated from the Maki formula [Eq. (3)]. Yasui and Kita⁵⁰ have made a detailed numerical investigation of the approximations used in many of the other previous superconducting state dHvA theories. They proposed an equation for R_{SC} which should give quantitative values for the energy gap which can be compared to the *actual* thermodynamic values. Their expression for R_{SC} is

$$R_{SC} = \exp\left[-2\pi\beta\left(\frac{\Delta_E(B)}{\hbar\omega_c}\right)^2\right], \quad (7)$$

where $\beta=0.0625$ is a numerically evaluated constant. This was shown to correctly describe the damping in Nb_3Sn and $NbSe_2$ with Δ_E approximately equal to the actual superconducting energy gap. It can be seen that this is almost exactly the same as Maki's formula, Eq. (3), except for a factor $2\beta/[\pi^{1/2}(F/B)^{1/2}]$ which equals 0.94 for $F=2700$ T and $B=15$ T. Hence, the gap values extracted by fitting this formula are virtually identical to those from Eq. (3), i.e., up to ten times larger than the gap values extracted by other means.

V. CONCLUSIONS

In conclusion, we have made a detailed study of the attenuation of the dHvA signal in MgB_2 as it enters the superconducting state. Only a single orbit on the electron-like π band is observable. The data clearly show that a sizeable gap exists on this orbit even at high field. The transition from normal to superconducting states as seen in both the background magnetization as well as the dHvA amplitude are rather broad, which may result from either fluctuation effects or a two-gap effect. The data provide a test for theories of the dHvA effect in the superconducting state being applied to a material which clearly has two superconducting gaps.

Both the Miyake and the Maki theories fit the data well, although the Miyake theory produces gap values which are much closer to those expected from the low field data for the π band. The most recent theoretical work^{50,58} however, suggests that the Miyake theory should seriously overestimate the damping and that the Maki model should provide an accurate quantitative estimate of the average gap on the dHvA orbit. Our data is in serious disagreement with this as

the gap values found from the Maki model fits are more than a factor 10 times larger than the expected zero field π band gap. We conclude that the present theories of the dHvA effect in the superconducting state, when applied to MgB₂, dramatically underestimate the damping.

ACKNOWLEDGMENTS

The authors would like to thank J. R. Cooper, S. M. Hayden, B. Györfy, T. Kita, and P. J. Meeson for useful discussions.

-
- ¹M. Iavarone, G. Karapetrov, A. E. Koshelev, W. K. Kwok, G. W. Crabtree, D. G. Hinks, W. N. Kang, E. M. Choi, H. J. Kim, H. J. Kim, and S. I. Lee, *Phys. Rev. Lett.* **89**, 187002 (2002).
- ²F. Bouquet, Y. Wang, R. A. Fisher, D. G. Hinks, J. D. Jorgensen, A. Junod, and N. E. Phillips, *Europhys. Lett.* **56**, 856 (2001).
- ³F. Bouquet, Y. Wang, I. Sheikin, T. Plackowski, A. Junod, S. Lee, and S. Tajima, *Phys. Rev. Lett.* **89**, 257001 (2002).
- ⁴F. Manzano, A. Carrington, N. E. Hussey, S. Lee, A. Yamamoto, and S. Tajima, *Phys. Rev. Lett.* **88**, 047002 (2002).
- ⁵S. Souma, Y. Machida, T. Sato, T. Takahashi, H. Matsui, S. C. Wang, H. Ding, A. Kaminski, J. C. Campuzano, S. Sasaki, and K. Kadowaki, *Nature (London)* **423**, 65 (2003).
- ⁶S. Tsuda, T. Yokoya, Y. Takano, H. Kito, A. Matsushita, F. Yin, J. Itoh, H. Harima, and S. Shin, *Phys. Rev. Lett.* **91**, 127001 (2003).
- ⁷L. Y. L. Shen, N. M. Senozan, and N. E. Phillips, *Phys. Rev. Lett.* **14**, 1025 (1965).
- ⁸G. Binnig, A. Baratoff, H. E. Hoenig, and J. G. Bednorz, *Phys. Rev. Lett.* **45**, 1352 (1980).
- ⁹J. Kortus, I. I. Mazin, K. D. Belashchenko, V. P. Antropov, and L. L. Boyer, *Phys. Rev. Lett.* **86**, 4656 (2001).
- ¹⁰A. Y. Liu, I. I. Mazin, and J. Kortus, *Phys. Rev. Lett.* **8708**, 087005 (2001).
- ¹¹H. J. Choi, D. Roundy, H. Sun, M. L. Cohen, and S. G. Louie, *Nature (London)* **418**, 758 (2002).
- ¹²A. Carrington and F. Manzano, *Physica C* **385**, 205 (2003).
- ¹³R. S. Gonnelli, D. Daghero, G. A. Ummarino, V. A. Stepanov, J. Jun, S. M. Kazakov, and J. Karpinski, *Phys. Rev. Lett.* **89**, 247004 (2002).
- ¹⁴P. Szabo, P. Samuely, J. Kacmarcik, T. Klein, J. Marcus, D. Fruchart, S. Miraglia, C. Marcenat, and A. G. M. Jansen, *Phys. Rev. Lett.* **87**, 137005 (2001).
- ¹⁵S. Graser, T. Dahm, and N. Schopohl, *Phys. Rev. B* **69**, 014511 (2004).
- ¹⁶T. Dahm (private communication).
- ¹⁷D. Daghero, R. S. Gonnelli, G. A. Ummarino, V. A. Stepanov, J. Jun, S. M. Kazakov, and J. Karpinski, *Physica C* **385**, 255 (2003).
- ¹⁸Y. Bugoslavsky, Y. Miyoshi, G. Perkins, A. Caplin, L. Cohen, A. Pogrebnnyakov, and X. Xi, *cond-mat/0307540* (2003).
- ¹⁹R. Gonnelli, D. Daghero, A. Calzolari, G. Ummarino, V. Delarocca, V. Stepanov, J. Jun, S. Kazakov, and J. Karpinski, *cond-mat/0308152* (2003).
- ²⁰R. Corcoran, P. Meeson, Y. Onuki, P. A. Probst, M. Springford, K. Takita, H. Harima, G. Y. Guo, and B. L. Györfy, *J. Phys.: Condens. Matter* **6**, 4479 (1994).
- ²¹R. Corcoran, N. Harrison, S. M. Hayden, P. Meeson, M. Springford, and P. J. Vanderwel, *Phys. Rev. Lett.* **72**, 701 (1994).
- ²²N. Harrison, S. M. Hayden, P. Meeson, M. Springford, P. J. Vanderwel, and A. A. Menovsky, *Phys. Rev. B* **50**, 4208 (1994).
- ²³N. J. Clayton, H. Ito, S. M. Hayden, P. J. Meeson, M. Springford, and G. Saito, *Phys. Rev. B* **65**, 064515 (2002).
- ²⁴M. Heinecke and K. Winzer, *Z. Phys. B: Condens. Matter* **98**, 147 (1995).
- ²⁵R. Settai, H. Shishido, S. Ikeda, Y. Murakawa, M. Nakashima, D. Aoki, Y. Haga, H. Harima, and Y. Onuki, *J. Phys.: Condens. Matter* **13**, L627 (2001).
- ²⁶Y. Inada, H. Yamagami, Y. Haga, K. Sakurai, Y. Tokiwa, T. Honma, E. Yamamoto, Y. Onuki, and T. Yanagisawa, *J. Phys. Soc. Jpn.* **68**, 3643 (1999).
- ²⁷H. Ohkuni, Y. Inada, Y. Tokiwa, K. Sakurai, R. Settai, T. Honma, Y. Haga, E. Yamamoto, Y. Onuki, H. Yamagami, S. Takahashi, and T. Yanagisawa, *Philos. Mag. B* **79**, 1045 (1999).
- ²⁸C. Bergemann, S. R. Julian, G. J. McMullan, B. K. Howard, G. G. Lonzarich, P. Lejay, J. P. Brison, and J. Flouquet, *Physica B* **230**, 348 (1997).
- ²⁹M. Hedo, Y. Inada, T. Ishida, E. Yamamoto, Y. Haga, Y. Onuki, M. Higuchi, and A. Hasegawa, *J. Phys. Soc. Jpn.* **64**, 4535 (1995).
- ³⁰D. Shoenberg, *Magnetic Oscillations in Metals* (Cambridge University Press, Cambridge, 1984).
- ³¹A. Wasserman and M. Springford, *Physica B* **194**, 1801 (1994).
- ³²H. Harima, *Physica C* **378**, 18 (2002).
- ³³H. Rosner, J. M. An, W. E. Pickett, and S. L. Drechsler, *Phys. Rev. B* **66**, 024521 (2002).
- ³⁴I. I. Mazin and J. Kortus, *Phys. Rev. B* **65**, 180510 (2002).
- ³⁵E. A. Yelland, J. R. Cooper, A. Carrington, N. E. Hussey, P. J. Meeson, S. Lee, A. Yamamoto, and S. Tajima, *Phys. Rev. Lett.* **88**, 217002 (2002).
- ³⁶A. Carrington, P. J. Meeson, J. R. Cooper, L. Balicas, N. E. Hussey, E. A. Yelland, S. Lee, A. Yamamoto, S. Tajima, S. M. Kazakov, and J. Karpinski, *Phys. Rev. Lett.* **91**, 037003 (2003).
- ³⁷Veeco Instruments Inc., Woodbury, New York; <http://www.veeco.com>
- ³⁸J. R. Cooper, A. Carrington, P. J. Meeson, E. A. Yelland, N. E. Hussey, L. Balicas, S. Tajima, S. Lee, S. M. Kazakov, and J. Karpinski, *Physica C* **385**, 75 (2003).
- ³⁹J. Karpinski, M. Angst, J. Jun, S. M. Kazakov, R. Puzniak, A. Wisniewski, J. Roos, H. Keller, A. Perucchi, L. Degiorgi, M. R. Eskildsen, P. Bordet, L. Vinnikov, and A. Mironov, *Supercond. Sci. Technol.* **16**, 221 (2003).
- ⁴⁰Z. D. Hao and J. R. Clem, *Phys. Rev. B* **43**, 7622 (1991).
- ⁴¹M. Angst, R. Puzniak, A. Wisniewski, J. Jun, S. M. Kazakov, J. Karpinski, J. Roos, and H. Keller, *Phys. Rev. Lett.* **88**, 167004 (2002).
- ⁴²M. Angst, R. Puzniak, A. Wisniewski, J. Roos, H. Keller, P. Miranovic, J. Jun, S. M. Kazakov, and J. Karpinski, *Physica C* **385**, 143 (2003).
- ⁴³A. Rydh, U. Welp, J. M. Hiller, A. E. Koshelev, W. K. Kwok, G. W. Crabtree, K. H. P. Kim, K. H. Kim, C. U. Jung, H. S. Lee, B.

- Kang, and S.-I. Lee, Phys. Rev. B **68**, 172502 (2003).
- ⁴⁴T. Terashima, C. Haworth, H. Takeya, S. Uji, H. Aoki, and K. Kadowaki, Phys. Rev. B **56**, 5120 (1997).
- ⁴⁵T. J. B. M. Janssen, C. Haworth, S. M. Hayden, P. Meeson, M. Springford, and A. Wasserman, Phys. Rev. B **57**, 11 698 (1998).
- ⁴⁶G. Goll, M. Heinecke, A. G. M. Jansen, W. Joss, L. Nguyen, E. Steep, K. Winzer, and P. Wyder, Phys. Rev. B **53**, R8871 (1996).
- ⁴⁷A. Carrington and J. Fletcher (unpublished).
- ⁴⁸E. Boaknin, M. A. Tanatar, J. Paglione, D. Hawthorn, F. Ronning, R. W. Hill, M. Sutherland, L. Taillefer, J. Sonier, S. M. Hayden, and J. W. Brill, Phys. Rev. Lett. **90**, 117003 (2003).
- ⁴⁹V. V. Guritanu, W. Goldacker, F. Bouquet, Y. Wang, R. Lortz, G. Goll, and A. Junod, cond-mat/0403590 (2004).
- ⁵⁰K. Yasui and T. Kita, Phys. Rev. B **66**, 184516 (2002).
- ⁵¹K. Maki, Phys. Rev. B **44**, 2861 (1991).
- ⁵²U. Brandt, W. Pesch, and L. Tewordt, Z. Phys. **201**, 209 (1967).
- ⁵³M. J. Stephen, Phys. Rev. B **45**, 5481 (1992).
- ⁵⁴K. Miyake, Physica B **188**, 115 (1993).
- ⁵⁵P. Miller and B. L. Gyorffy, J. Phys.: Condens. Matter **7**, 5579 (1995).
- ⁵⁶This scaling is found both experimentally and in band-structure calculations.³²
- ⁵⁷I. I. Mazin, O. K. Andersen, O. Jepsen, A. A. Golubov, O. V. Dolgov, and J. Kortus, Phys. Rev. B **69**, 056501 (2004).
- ⁵⁸K. P. Duncan and B. L. Gyorffy, J. Phys.: Condens. Matter **15**, 239 (2003).